Processing on Gravity Anomaly Map of East Zhejiang Province by Means of Wavelet Analysis

Jun Chen, Bo He
School of Ocean and Earth Science
Tongji University
Shanghai, China
junxianchen@tongji.edu.cn

Zongxiu Wang, Chunlin Li
Institute of Geomechanics
Chinese Academy of Geological Sciences Beijing, China

Abstract— **The changes of trend and character of the gravity anomaly map can be used to interpret the fault distribution. The gravity anomaly map of east Zhejiang province had been decomposed by means of wavelet analysis. The wavelet details maps show that the faults can be divided into 3 levels from the aspects of scale and depth. The 1st level faults are NE-SW directional faults, which have big extension length and depth. Most of them have outcropped. The 2nd level faults are NW-SE directional faults, which have small depth, some of them have outcropped, but most of them are concealed, and cut the NW-SE faults. The 3rd level faults are approximately S-N directional faults. Those are concealed and covered by NW-SE faults, so they formed earlier than NW-SE faults. In the southern section, there is a big granite, which forked toward the ground, and scattered on the earth's surface. The results above demonstrated that the information of different objective density resources can be extracted effectively from the gravity anomaly map through wavelet analysis.**

Keywords—***Digital image processing; Gravity anomaly map; Wavelet analysis; Zhejiang province; Information extraction***

I. Introduction

Digital image may be usually the superimposition results of different type useful or useless information. Such as the noise disturbance during data acquisition or data transmission, and the information superimposition of different scale objects. It is one of the research contents for digital image processing to extract the objective information from the digital image for one specially appoint ed research object.

The gravity anomaly is closely allied to the density distribution of material which forming the earth's crust. In the general case, the gravity anomalies are the superimposition of all kinds of geological factors. The bulk effect is one of the important characters for the gravity anomaly. The values and shapes of gravity anomaly are the comprehensive results of different depth and different scale density resources. So the gravity anomaly map is very complicated. The interpretation of the gravity anomaly map is to get the depth, shape and density information from its information of anomaly characters. The changes of positive or negative values and the increasing or decreasing trend often reflects the rising or falling trend of new or old stratum. The gravity gradient may reflect the fault or the fault belt, the fracture belt, the contact zone between different density rocks, stratum bending, and so on. According to the gravity frequency analysis, the lower frequency information reflect the deeper or the bigger scale density resources, but the higher frequency information reflect the shallower or smaller scale density resources. In order to recognize the anomaly character accurately, it is the key step to separate the mix information and extract the objective information.

Wavelet transform is developed in the 1990s. It is one tool for applied mathematics, which is one multi-scale time-frequency analysis tool based on Fourier transform and Gabor transform. It has good local analytic properties in both frequency domain and spatial domain [1]. And it has been widely used for image processing and signal processing [2,3]. In recent decades, it has also been used for gravity anomaly image processing, such as anomaly filtering, weak information analysis, and anomaly separation. There in particular have been many researches on separation of potential

anomalies and border detection of buried structures using wavelet approaches [4]. Hou and Yang for the first time applied wavelet transformation and multi-scale methods on gravity anomalies in China [5]. Fedi and Quata had separated regional and residual potential-field anomalies using the wavelet transform [6]. Hornby et al. has separated potential anomaly data by wavelet approach [7]. Liang and Zhang had obtained the residual anomaly related with igneous rock and deep fault through wavelet transform [8]. Chen and Sun had obtained the information on the evolution of the boundary faults through the comparison between the Bouguer anomaly map and different order wavelet details map [9].

II. Wavelet analysis

The main idea of wavelet analysis is to decompose the spatial domain into a series of sub-spaces with different resolutions. The most common arithmetic applied to wavelet analysis is the pyramid decomposition and reconstruction algorithm. The importance of it can be compared as Fast Fourier Transform in Classic Fourier Analysis [10]. In 1989, Mallat presented the multi-resolution analysis conception and gave the classic orthogonal wavelet fast algorithm: Mallat algorithm. Firstly, the signals are divided into two parts, higher frequency part and lower frequency part. Then the lower frequency part is divided continuously. The 2nd step is repeated till meeting the scheduled requirements of the signal treatment. It has higher frequency resolution for the low frequency signals.

If $(V_j)_{jez}$ is one dimensional multi-scale analysis, the scale function $\phi(x)$ and wavelet function $\psi(x)$ of function $f(x,y)$ in two dimensional plane meet two scale equation. $(V_j^2)_{jez}$ forms one two dimensional multi-scale analysis when $V_j^2 = V_j \oplus V_j$ [11,12]. The scale function is

$$\phi(x,y) = \phi(x) \bullet \phi(y), \tag{1}$$

and the wavelet functions are

$$\begin{cases} \psi^1 f(x,y) = \psi(x) \bullet \phi(y) \\ \psi^2 f(x,y) = \phi(x) \bullet \psi(y) \\ \psi^3 f(x,y) = \psi(x) \bullet \psi(y) \end{cases} \tag{2}$$

when $f(x,y) \in (V_j^2)_{jez}$, $\psi^1 f(x,y)$, $\psi^2 f(x,y)$, $\psi^3 f(x,y)$ are wavelet function in horizontal, vertical and diagonal line direction respectively.

If $Af(x,y)$ denotes wavelet approximation and $Df(x,y)$ denotes wavelet details, $Af(x,y)$ is the lower frequency or big scale information, and $Df(x,y)$ is the high frequency or small scale information.

$$f(x,y) = A_0 f(x,y) \tag{3}$$

$$A_j f(x,y) = A_{j+1} f(x,y) + \sum_{\varepsilon=1}^{3} D_{j+1}^{\varepsilon} f(x,y) \tag{4}$$

$$A_{j+1} f(x,y) = \sum_{m_1,m_2 \in z} s_{m_1,m_2}^{j+1} \phi_{m_{m_1,m_2}}^{j} \tag{5}$$

$$D_{j+1}^{T} f(x,y) = \sum_{m_1,m_2 \in z} d_{m_1,m_2}^{j+1,T} \phi_{m_1,m_2}^{j,T} \tag{6}$$

$$\begin{cases} s_{m_1,m_2}^{j+1} = \sum_{k_1,k_2 \in z} h_{k_1-2m_1} h_{k_2-2m_2} s_{m_1,m_2}^{j} \\ d_{m_1,m_2}^{j+1,1} = \sum_{k_1,k_2 \in z} h_{k_1-2m_1} g_{k_2-2m_2} s_{m_1,m_2}^{j} \\ d_{m_1,m_2}^{j+1,2} = \sum_{k_1,k_2 \in z} g_{k_1-2m_1} h_{k_2-2m_2} s_{m_1,m_2}^{j} \\ d_{m_1,m_2}^{j+1,3} = \sum_{k_1,k_2 \in z} g_{k_1-2m_1} g_{k_2-2m_2} s_{m_1,m_2}^{j} \end{cases} \tag{7}$$

here

$$h_k = \tfrac{1}{\sqrt{2}} \int_{-\infty}^{\infty} \phi(\tfrac{x}{2}) \overline{\phi(x-k)} dx \tag{8}$$

$$g_k = (-1)^{k-1} h_{1-k} \tag{9}$$

The larger the coefficient j is, the deeper the source depth will be. The smaller the coefficient j is, the shallower the field sources related to the anomalies will be. According to the above principle, the gravity $\Delta g(x,y)$ can be expressed as

$$\Delta g(x,y) = A_n \Delta g(x,y) + \sum_{j=1}^{n} D_j \Delta g(x,y) \tag{10}$$

after it was decomposed n times.

III. Processing result of the gravity anomaly map

A. *Gravity data*

Here the gravity anomaly data is the Bouguer gravity data, and is provided by the Institute of Geomechanics. The gravity data is generated using the kriging method to interpolate data with a grid interval

1km x 1km. The coordinate system is 123° of central meridian and Beijing 54 of elevation system.

The obvious character of the gravity anomaly map (Fig.1 a) is that most of the gravity values are negative. The values are between -85mGal to 30mGal. The minimum value is near Longquan, which is in the southwestern part. The maximum value is to the northeast of Cixi. The main anomalous direction is northeast. And the anomaly values increase gradually from southwest to northeast, which illustrated that the Bouguer gravity anomalies reflected the deeper structural character. It can be divided into two parts. The northwestern part has obvious linear character, and the main direction is NE-SW. The values are bigger than -30mGal. But the anomaly direction in the southeastern zone is not obvious. The values are smaller then -25mGal. The independent anomaly circles have the overall anomaly shape becoming complex. Most of the independent anomaly traps are in the direction of northeast.

B. Processing results

In order to interpret the anomaly character changes with the depth, here we have calculated the 1st -5th order gravity wavelet details (Fig1.b-f). With the order varying from the 1st to 5th, the anomalies related to faults and any other minor structural units vanished gradually, with only the deeper macroscopic anomalies left.

The distribution and shape of the positive (white) and negative (grey) anomalies are different in gravity details map with different order.

The positive gravity anomaly values have apparent NW-SE direction in the 1st order wavelet details map (Fig.1 b) and the 2nd order wavelet details map (Fig.1 c). There is one obvious boundary along Jiangsha, Jinhua, Zhuji to Shaoxing. In the northwestern part the main anomaly directions are NE-SW. But they are not continuous. In the southeastern part the main anomaly directions are NW-SE. The NW-SE direction anomalies decrease gradually from the 1st order to the 2nd order. These reflect that there are NW-SE faults, and they mainly exist in southeastern Zhejiang province.

In the 3rd order wavelet details map (Fig.1 d), the main character of the northwest part is linear trend of NE-SW direction. The southeastern part has no obvious linear character. But in the southern section there is one typical circle negative anomaly, and it is surrounded by positive anomalies at Longquan. It indicates that the distribution of faults is more complicated in southeastern region than that in northwestern region.

The main direction trend of the 4th order wavelet details map (Fig.1 e) is similar with the 3rd order wavelet details map. But the anomalies are more wide and gentle in the 4th order wavelet details map than that in the 3rd order wavelet details map. In the respect of frequency, the 3rd order wavelet details map have more high frequency anomalies than the 4th order wavelet details map. Some of the main faults include a series of parallel small faults in shallow depth, and the small faults vanished gradually with the increasing of depth. The existence of ring-shaped anomaly, the negative anomalies circled by positive anomalies, displays the existence of granite.

The 5th order wavelet details map (Fig.1 f) presents four directions of linear anomalies, such as northeast -southwest, northeast-southwest, east-west and south-north. In the same time, the northeast-southwest direction anomalies are cut by northwest-southeast or norheast-southeast direction anomalies. The boundary along Jiangshan, Jinhua, Zhuji to Shaoxing is still the obvious character, which divides the anomaly map into two sections, that is northwestern section and southeastern section.

Comparing the details maps with each other, in the southern section the scattered gravity lows in lower details maps become gradually one negative anomaly circle. It demonstrates that the scattered granite outcrops connect with each other as the depth increasing, and become one bigger granite.

IV. Conclusions

The gravity anomalies map is the superimposition result of faults (directional anomaly or distortional deformation), igneous rock (circle anomaly) and some other density resources. The anomaly with different depth and scale can be separated through wavelet analysis.

In east Zhejiang province, the Bouguer gravity anomaly reflected mainly the deeper structural character. The main fault direction is NE-SW, and this group of faults has bigger depth and length. And we can track its information from 1st order to 5th order wavelet details

map. Both of the scale and depth of NW-SE faults are smaller than that in NE-SW direction, which are reflected only in 1st order and 2nd order wavelet maps. And it faded gradually in 2nd order and 3rd order wavelet maps. There are concealed S-N faults in the deep, this character becomes more and more obvious from 4th order to 5th order wavelet details map. And they are covered by NW-SE faults, so they formed earlier than NW-SE fault.

Acknowledgements

We would like to thank the China Geological Survey for financial support (Geological survey project N0. 1212011121068). We also thank the anonymous editors and reviewers for their suggestions, which improved the manuscript.

References

[1] H. Zhang and Y. Wu, Application of wavelet packet in gravity anomaly processing, Global Geology, vol.15(2) (2012), pp.187-190

[2] Arvind R. Yadav, R.S. Anand, M.L. Dewal, Sangeeta Gupta, Multiresolution local binary pattern variants based texture feature extraction techniques for efficient classification of microscopic images of hardwood species, Applied Soft Computing, Vol. 32 (2015), pp. 101-112

[3] A. Rahmati, R. Adhami, M. Dimassi, Real-time electrical variables estimation based on recursive wavelet transform, International Journal of Electrical Power & Energy Systems, Vol. 68 (2015), pp. 170-179

[4] Alp Hakan, A. Muhittin Albora and Tur Huseyin, A view of tectonic structure and gravity anomalies of Hatay Region Southern Turkey using wavelet analysis, Journal of Applied Geophysics, vol. 75 (2011), pp. 498-505

[5] Z. Z. Hou, W. C. Yang, Wavelet transform and multi-scale analysis on gravity anomalies of China, Journal of Geophysics, vol. 40(1)(1997),pp.85-95

[6] M. Fedi and T. Quata, Wavelet analysis for the regional-residual and local separation of potential field anomalies, Geophys. Prospect. Vol.46(1998), pp.507-525

[7] P. Hornby, F. Boschetti, F.G. Horovitz, Analysis of potential field data in the wavelet Domain. Geophys. J. Int. vol.137 (1999), pp.175-196

[8] X. LIANG and M. L. ZHANG, Application of 2D Wavelet Multi-scale Analysis on Depth Mineral Deposit Exploration at Tongshankou, Resources Environment & Engineering, vol.26(3)(2012), pp.263-267.

[9] J. Chen, L. P. Sun, Z. Y. Zhou and Y. J. Chen, Wavelet Analysis Results of Gravity Anomalies and Its Geological Significance in Hefei Basin, Journal of Tongji University (Natural Science), vol.33(9)(2005), pp.1244-1247

[10] W. L. Jiang, J. F. Zhang, T. Tian and X. Wang, Crustal structure of Chuan-Dian region derived from gravity data and its tectonic implications, vol. 212(2012), pp.76-87

[11] D. H. Li，Q. He, C. M. Li and J. H. Qu, Research on Wavelet Analysis Method of Aeromagnetic Anomaly Extraction based on MATLAB and C+ + Mixed Programming, Journal of Seismological research, vol.34(2)(2011), pp.233-238

[12] D. Z. Gao, Z. Z. Hou, J. Tang, Multi-scale analysis of gravity anomalies on East China Sea and adjacent regions, Chinese Journal of Geophysics, vol.43(6) (2000), pp.842-849

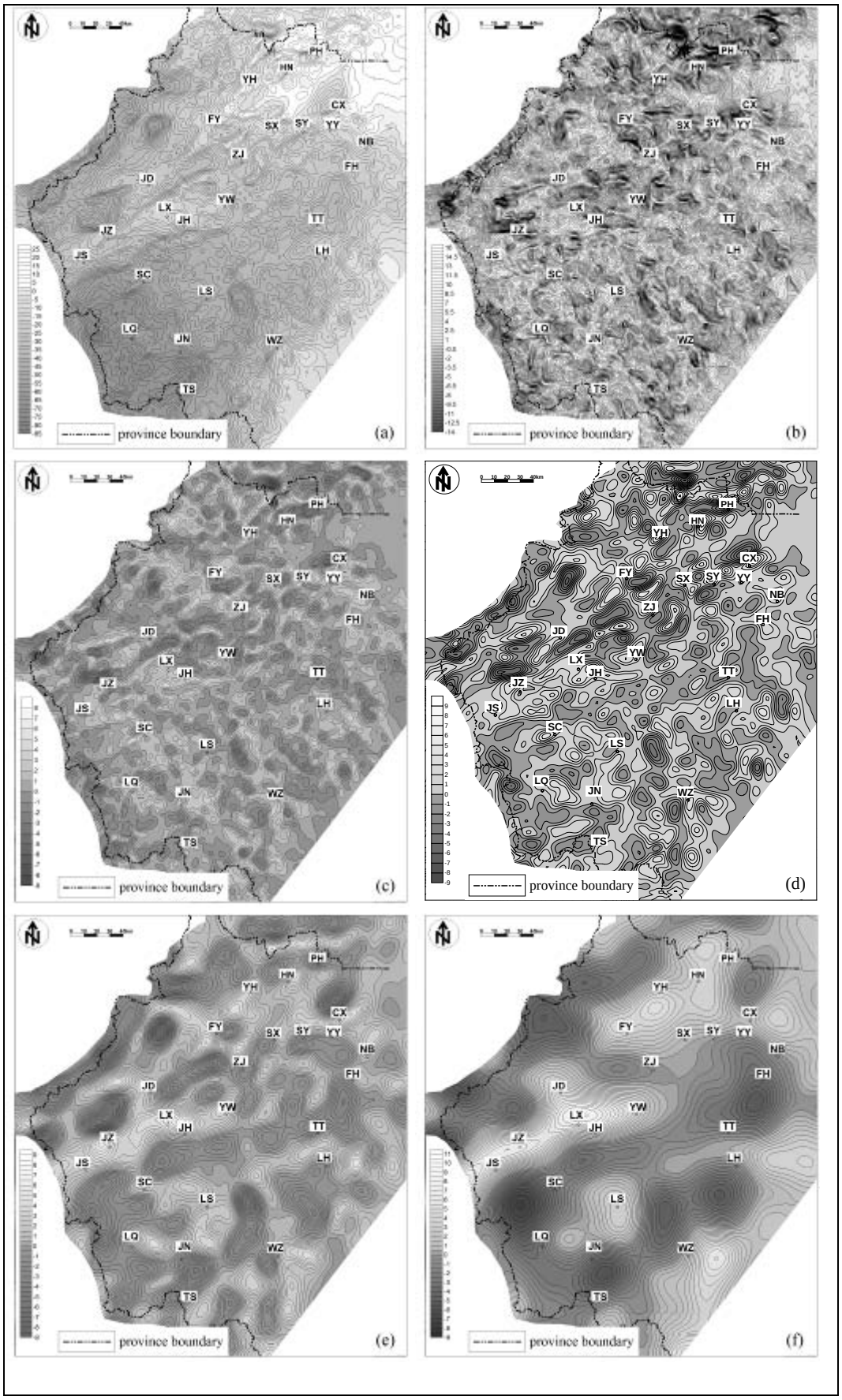

Figure 1. The gravity anomaly map(a) and its wavelet details map(b.1st order, c.2nd order, d.3rd order. e.4th order and f.5th order) of east Zhejiang (PH-Pinghu, CX-Cixi, YY-Yuyao, YH-Yuhang, SH-Shaoxing, NB-Ningbo, FY-Fuyang, ZJ-Zhuji, HN-Haining, SY-Shangyu, FH-Fenghua, YW-Yiwu, JH-Jinhua, JD-Jiande, TT-Tiantai, LH-Linhai, LX-Lanxi, JZ-Juzhou, JS-Jiangshan, SC-Suichang, LS-Lishui, LQ-Longquan, TS-Taishun, JN-Jingning, WZ-Wenzhou)